

Original Research

A Numerical Investigation of Nutrient Concentrations in Gdańsk Gulf as Revealed by a Coupled One-Dimensional Model

L. Dzierzbicka-Głowacka*

Institute of Oceanology, Polish Academy of Sciences, Powstańców Warszawy 55, PL-81-712 Sopot, Poland

Received: February 1, 2005

Accepted: May 19, 2005

Abstract

A dynamics model for nutrients was coupled with a one-dimensional physical and biological upper layer model to simulate the temporal changes not only in distributions of a nutrient but then of phytoplankton and zooplankton and study the role of these biological characteristics in the dynamics of the Gdańsk Gulf ecosystem. The 1D model consists of three submodels: a meteorological submodel for the physics of the upper layer and a biological submodel, which also is driven by output from the physical submodel. The biological upper layer model {*nutrient-phytoplankton-zooplankton-detritus*} incorporates formulations of the primary production mechanism and of the remineralization mechanisms within the mixed layer, in the lower layers and at the bottom as well as of the daily migration of zooplankton mechanism. The model is based on total inorganic nitrogen ($\text{NO}_3 + \text{NO}_2 + \text{NH}_4$) and phosphate (PO_4).

The calculations were made for 180 days (from March to August) for two stations at Gdańsk Gulf (at station A, near the Vistula river mouth, and at station B, located further to the open sea). The results of the numerical investigations described here were compared with the mean observed values of characteristics investigated for 10 years, 1990-2000. Comparison of computed and measured values shows the model reproduces the time-vertical structure of characteristics investigated in accordance with the *in situ* observations. The numerical simulations shown that the differences between the simulated and mean observed values of nutrient in the upper layer are c. 1 mmol m⁻³ for total inorganic nitrogen and 0.1 mmol m⁻³ for phosphate. The slight differences between the calculated and observed values of surface chlorophyll-*a* and microzooplankton biomass are ca. 5-20%, depending on the location of the hydrographic station and the month for which the calculations were made. The model can be used to describe the temporal patterns for nutrients distributions and phytoplankton and zooplankton biomass.

Keywords: nutrient, phytoplankton, zooplankton, model, Gdańsk Gulf

Introduction

The complexity of the hydrophysical and biological processes in the marine environment and the links between these processes require modern techniques, i.e. mathematical modelling and computer simulations, for

their study. Although field work provides the most reliable information on these mechanisms and processes, it requires comprehensive and costly *in situ* observations conducted under a variety of hydrological conditions for long periods of time. They are nevertheless essential for the collection of sufficient statistical data sets for an adequate diagnosis of the state of the environment and for making forecasts.

*e-mail: dzierzb@iopan.gda.pl

Computer experiments permit a considerable reduction in costs, because model studies enable different hydrological situations to be simulated and hypotheses and assumptions concerning the mechanisms to be tested. As opposed to *in situ* measurements, such model studies can be repeated several times. The simulation results provide fresh data sets. On this basis, new tasks for field studies can be specified, and new hypotheses or theoretical models concerning processes or separate mechanisms can be formulated.

To some extent, of course, mathematical modelling is limited by the available knowledge of particular processes, the methods used to parameterize the links between them and the possibilities of realizing them in the model. This explains the present widespread use of mathematical models and computer simulations as tools lead in to the discovery of natural laws. They are used in particular to solve problems of an interdisciplinary nature, which is what oceanographic studies usually are.

Marine system modelling is a superior way to formalize and test knowledge about a complex aquatic ecological system and to seek means for the rational management of our living marine resources. A marine system model is comprised of two parts: hydrodynamic and ecosystem. The equations are in a developing stage.

The hydrodynamic models have been developed for the Baltic Sea during the last 30 years. A review of Baltic Sea hydrodynamic modelling has been given by [1, 2, 3, 4]. A good review of coastal marine ecosystem modelling

has been published by [5-9] for North Sea. The ecological modelling of the Baltic Sea began at the end of the 1960s with material balances models [10]. The first general conceptual ecosystem model of the Baltic Sea was presented by [11]. Practical simulations of the Baltic Sea ecosystem are made by [4, 12-16] and here particularly should be included models with a high-resolution zooplankton module [17, 18, 19]. These papers present population dynamics of *Calanus finmarchicus* and *Pseudocalanus elongatus*. However, a model of copepod growth and development was presented by [20, 21].

Here, I present the structure with mathematical description of a coupled 1D-ecosystem model of upper layer. This model consists of three submodels: meteorological, physical and biological. The biological submodel consists of five mass conservation equations. There are four diffusion advection reaction equations for phytoplankton and zooplankton and a double nutrient in the water column. The fifth equation, an ordinary differential equation, describes the development of detritus at the bottom. The 1D-model has been used to investigate numerically the nutrient dynamics in the Gdańsk Gulf.

1D Ecosystem Model

An one-dimensional ecosystem model consists of three submodels: a meteorological submodel for the physics of the

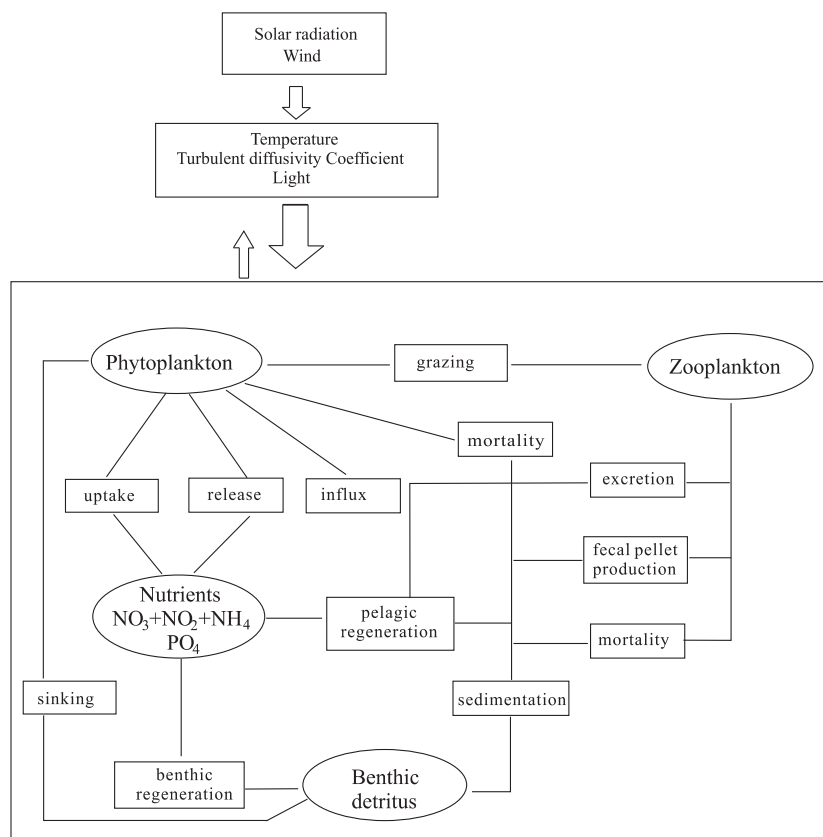


Fig. 1. Conceptual diagram of the coupled model.

upper layer and a biological submodel, which also is driven by output from the physical submodel (see Figure 1).

Meteorological Submodel

The meteorological component calculates the forcing functions for the physical oceanographic and biological components. Wind stress, τ_u and τ_v , global radiation, Q_p , and the heat balance at the sea surface, Q , are determined from standard meteorological data and hydrographic climatological data. Global radiation, Q_p , is calculated by application and adaptation of a radiation model, which is based on the radiation at the outer atmosphere and local cloudiness. The latent, Q_L , and sensible, Q_S , heat fluxes are calculated by so-called bulk formulae.

Physical Submodel

I consider here the dynamics of the horizontally quasi-homogeneous upper layers of the ocean in terms of ocean boundary layer dynamics. Thus all horizontal gradients vanish. The Coriolis force is maintained to enable Ekman layer dynamics. Both velocities, u and v , are affected by turbulent diffusion, A_z , and Coriolis acceleration, f . Temperature, T , changes are caused by turbulent heat diffusion, A_z , and solar heating of the water column and the surface heat fluxes, Q_p , [23, 24].

$$\frac{\partial u}{\partial t} - fv = \frac{\partial}{\partial z} \left(A_z \frac{\partial u}{\partial z} \right) \quad (1)$$

$$\frac{\partial v}{\partial t} - fu = \frac{\partial}{\partial z} \left(A_z \frac{\partial v}{\partial z} \right) \quad (2)$$

$$\frac{\partial T}{\partial t} = \frac{\partial}{\partial z} \left(A_z \frac{\partial T}{\partial z} - \frac{1}{c\rho_0} Q_L e^{-K_d z} \right) \quad (3)$$

The turbulent diffusion in these equations which denotes the vertical eddy coefficient for momentum and heat is obtained by [22] as:

$$A_z = 5 \times 10^{-4} (1 + Ri)^{-1.5} + 2 \times 10^{-5} \quad (4)$$

where Ri is the Richardson number.

Boundary Conditions

The boundary conditions for momentum transfer across the sea surface are:

$$F_u(0) \equiv A_z \frac{\partial u}{\partial z} \Big|_{z=0} = -\frac{\tau_u}{r_0}, F_v(0) \equiv A_z \frac{\partial v}{\partial z} \Big|_{z=0} = -\frac{\tau_v}{r_0} \quad \text{at } z=0 \quad (5)$$

Wind stress in x- and y-direction is denoted as τ_u and τ_v , respectively. The total heat flux Q at the sea surface is

transmitted according to:

$$F_H(0) \equiv c\rho A_z \frac{\partial T}{\partial z} \Big|_{z=0} = Q_I - Q_B + Q_L + Q_S = Q \quad \text{at } z=0 \quad (6)$$

The heat and radiation fluxes Q carry the indices B for long-wave back-radiation, S for sensible heat flux, and L for latent heat flux.

At the bottom the velocity components vanish and the heat flux is vanishing:

$$u = v = 0 \quad \text{at } z = 0 \quad (7)$$

$$\frac{\partial T}{\partial z} = 0 \quad \text{at } z = 0 \quad (8)$$

Biological Submodel

The biological submodel comprises a five-state variable: nutrient (total inorganic nitrogen and phosphate), phytoplankton, zooplankton and detritus on the bottom (Fig. 1). The equations, process formulations and parameter values used here are similar to those described in [16, 19].

My philosophy is to make the model as simple as possible, so I model phytoplankton by only one state variable, represented by the carbon concentration. The model is based on total inorganic nitrogen ($NO_3 + NO_2 + NH_4$) and phosphate (PO_4). The nutrient serves both as a trigger and as a limiting agent for primary production. I use a constant Redfield ratio. The concept of the detrital pool at the bottom has been introduced to create a lag in remineralization of the majority of detritus and the eventual replenishment of the upper layer with nutrients. This complex process is parameterized by assuming a net remineralization rate for bottom detritus. The zooplankton has been introduced into the 1D-model as a biomass and is represented by microzooplankton.

The phytoplankton standing stock, zooplankton and nutrient in the water column serve as time- and depth-dependent pools. Detritus is a time dependent pool at the bottom. All four pools are prognostic state variables. Bacteria are not explicitly simulated as prognostic variables. Their activity only appears implicitly in the parameterizations of the remineralization terms. Benthic detritus accumulates by sinking out the water column. It is regenerated by bacterial action, and the resulting nutrient diffuses upwards by turbulent diffusion.

The system of equations consists of five nonlinearly coupled partial differential equations of second order for phytoplankton, zooplankton and two for nutrients and one ordinary differential equation of first order for benthic detritus.

The changes in local nutrient concentration (for total inorganic nitrogen and phosphate) $Nutr$ is determined by turbulent diffusion K_z , algal uptake UPT , nutrient influx F_{inP} , remineralized dead phytoplank-

ton, zooplankton faecal pellets and dead zooplankton REMI, and by zooplankton excretion EXC and nutrient release REL.

$$\frac{\partial \{Nutr_N\}}{\partial t} = \frac{\partial}{\partial z} \left(K_z \frac{\partial \{Nutr_N\}}{\partial z} \right) - \text{UPT}_N + F_{\text{inf}N} + \text{REL}_N + \text{REMI}_N + \text{EXC}_N \quad (9)$$

$$\frac{\partial \{Nutr_P\}}{\partial t} = \frac{\partial}{\partial z} \left(K_z \frac{\partial \{Nutr_P\}}{\partial z} \right) - \text{UPT}_P + F_{\text{inf}P} + \text{REL}_P + \text{REMI}_P + \text{EXC}_P \quad (10)$$

The temporal changes in the phytoplankton biomass *Phyt* is affected by turbulent diffusion K_z , sinking of algae w_z , primary production PRE, respiration RES, mortality MOR_p and grazing by zooplankton GRA.

$$\frac{\partial \{Phyt\}}{\partial t} + w_z \frac{\partial \{Phyt\}}{\partial z} = \frac{\partial}{\partial z} \left(K_z \frac{\partial \{Phyt\}}{\partial z} \right) + \text{PRE} - \text{RES} - \text{MOR}_p - \text{GRA} \quad (11)$$

The temporal changes in the local zooplankton biomass concentration *Zoop* are defined by turbulent diffusion K_z , ingestion ING, zooplankton faecal pellets FEC, metabolism MET and predation (=mortality) PRED.

$$\frac{\partial \{Zoop\}}{\partial t} = \frac{\partial}{\partial z} \left(K_z \frac{\partial \{Zoop\}}{\partial z} \right) + \text{ING} - \text{FEC} - \text{MET} - \text{PRED} \quad (12)$$

Finally, the temporal changes in the detritus pool at the bottom *Detr* are determined by the flux of phytoplankton F_p and that of detrital material sedimenting out of the water column onto the bottom D and remineralisation of detritus REMD.

$$\frac{d\{Detr\}}{dt} = -F_p(H) + D - \text{REMD} \quad (13)$$

The turbulent diffusion coefficient K_z (used in above equations) is determined after [22] as:

$$K_z = 5 \times 10^{-4} (1 + Ri)^{-2.5} + 10^{-6} \quad (14)$$

The biochemical terms used in Eqs. (9)-(13) are given in the Appendix. The significance of symbols used is given in Table 1. However, the dynamical constants used in the biological model are listed in Table

2. The detailed descriptions of the processes having the influence on the source/sink function are presented in the work of [16].

Initial and Boundary Conditions

The following initial and boundary conditions supplement equation system (9)-(13): the initial vertical distributions of phytoplankton $\{Phyt\}$, nutrient $\{Nutr\}$, zooplankton $\{Zoop\}$ and detritus pool $\{Detr\}$ are known:

$$\begin{aligned} \{Phyt\}(z, 0) &= \{Phyt\}_0(z) & 0 \leq z \leq H \\ \{Zoop\}(z, 0) &= \{Zoop\}_0(z) & 0 \leq z \leq H \\ \{Nutr_N\}(z, 0) &= \{Nutr_N\}_0(z) & 0 \leq z \leq H \\ \{Nutr_P\}(z, 0) &= \{Nutr_P\}_0(z) & 0 \leq z \leq H \\ \{Detr\}(t = 0) &= \{Detr\}_0 = 0 & z = H \end{aligned} \quad (15)$$

The vertical gradient of phytoplankton, zooplankton and nutrient concentration flux are zero at the sea surface ($z = 0$):

$$\begin{aligned} F_p(0) &\equiv K_z \frac{\partial \{Phyt\}(z, t)}{\partial z} \Big|_{z=0} - w_z \{Phyt\}(0, t) = 0 \\ F_{N_N}(0) &\equiv K_z \frac{\partial \{Nutr_N\}(z, t)}{\partial z} \Big|_{z=0} = 0 \\ F_{N_P}(0) &\equiv K_z \frac{\partial \{Nutr_P\}(z, t)}{\partial z} \Big|_{z=0} = 0 \\ F_Z(0) &\equiv K_z \frac{\partial \{Zoop\}(z, t)}{\partial z} \Big|_{z=0} = 0 \end{aligned} \quad (16)$$

However, the bottom flux condition for phytoplankton, nutrient and zooplankton is given as:

$$F_p(H) \equiv -w_z \{Phyt\}(H, t) \quad (17)$$

$$F_{N_N}(H) \equiv K_z \frac{\partial \{Nutr_N\}(z, t)}{\partial z} \Big|_{z=H} = g_N \text{REMD} \quad (18)$$

$$F_{N_P}(H) \equiv K_z \frac{\partial \{Nutr_P\}(z, t)}{\partial z} \Big|_{z=H} = g_P \text{REMD}$$

$$F_Z(H) \equiv K_z \frac{\partial \{Zoop\}(z, t)}{\partial z} \Big|_{z=0} = 0 \quad (19)$$

Table 1. List of symbols used in Appendix.

Symbol	Meaning
K_z	Turbulent diffusion coefficient
g_N	C/N ratio
g_P	C/P ratio
g_{Chl}	C/Chl- <i>a</i> ratio
$\{Phyt\}$	Phytoplankton biomass
d_A	Assimilation number
E_o	Saturation irradiance
E	Irradiance at depth z
η_d	Average daily doses of irradiation PAR
$\{Phyt\}_o$	Phytoplankton threshold for grazing
g_{max}	Maximum grazing rate
k_{Phyt}	Half-saturation constant for grazing
m_P	Mortality rate for $\{Phyt\}$
m_P^n	Percentage basic respiration
m_P^d	Percentage photorespiration
$\{Nutr\}_N$	Total inorganic nitrogen concentration
$\{Nutr\}_P$	Phosphate concentration
k_{Nutr}	Half-saturation constant for nutrient (N and P)
n_e	Percentage of ingestion regenerated as soluble excretion of zooplankton
n_f	Percentage of ingestion egested as fecal material
n_z	Percentage of ingestion ending finally as dead zooplankton
p_f	Percentage of remineralized fecal material in the water column
p_P	Percentage of remineralized dead organic matter in the water column
p_z	Percentage of remineralized dead zooplankton in the water column
$\{Zoop\}$	Zooplankton biomass
fil	Maximum ingestion food
m_z	Mortality rate for $\{Zoop\}$
$\{Detr\}$	Detritus concentration
r_d	Remineralization rate of benthic detritus

This flux $F_p(H)$ enters the benthic detritus equation as a source term. The boundary condition [18] provides the mechanism of replenishing the water column with nutrients resulting from benthic remineralization.

The system of equations with initial and boundary conditions is solved numerically by using the indirect Crank-Nicholson method [25] in an area of $0 \leq z \leq H$ by digitizing this region with a variable step. This method is a second-order one, absolutely stable at every time and space step. The detailed algorithm of the solution to 1D-biological model can be found in [16].

Numerical Simulations

The aim is not generality but a description of a numerical investigation of nutrient dynamics in one example of a model. The temporal changes in distributions of a nutrient (inorganic nitrogen, and phosphate), of phytoplankton carbon and of zooplankton are necessary outputs from the biological model. The calculations were made for 180 days (from March to August) for two stations at Gdańsk Gulf (at station A, near the Vistula river mouth, and at station B located further to the open sea

Table 2. Dynamical constants in the biological model.

Symbol	Value	Unit
g_{\max}	0.5	day ⁻¹
g_N	0.0157	mmol N (mg C) ⁻¹
g_P	0.612×10^{-3}	mmol P (mg C) ⁻¹
g_{Chl}	34.31	mg C (mg Chl) ⁻¹
k_{Phyt}	100	mg C m ⁻³
k_{NutrN}	0.1	m mol N m ⁻³
k_{NutrP}	0.06	m mol P m ⁻³
m_p	0.05	day ⁻¹
m_p^n	0.1	
m_p^d	0.05	
n_e	0.33	
n_f	0.33	
n_z	0.33	
p_f	0.2	
p_p	0.2	
p_z	0.2	

– see Fig. 2). Initial values of characteristics investigated as constants with depth were assumed on the basis interpolation of empirical data, i.e. $Nutr_N = 8$ and 6 mmol m⁻³, $Nutr_P = 0.7$ and 0.6 mmol m⁻³, $Phyt = 50$ mgC m⁻³, $Zoop = 2$ and 1 mgC m⁻³ and $Detr = 0$ mgC m⁻², respectively at stations A and B.

The flow field and water temperature used as the inputs of the biological submodel were reproduced by the physical submodel. Both velocities and temperature resulting from the physical submodel (as the output) were used for the turbulent diffusion calculation. However, temperature data was also used for the primary production calculation. Comparison of computed and measured temperatures shows the model reproduces the vertical structure of seawater temperature in relatively good accordance with the *in situ* observations (see for comparison - data from literature [26]). The temperature distributions at stations A and B are different (Fig. 3). The water temperature is about 2°C higher at station A than at station B in the upper layer. However, in the lower layer it is nearly the same for both stations.

The differences between the calculated and observed values of surface temperature are ca. 1-2°C, depending on the location of the hydrographic station (Fig. 4). For example, in the upper layer, the simulated temperature is equal to ca. 20°C at A and ca. 18°C at B late August; however, observed values were ca. 2°C lower than calculated.

Samples of inorganic nitrogen compounds (nitrates, nitrites and ammonia) taken from water were collected in determined layers: 0- 15 m (euphotic layer, above the seasonal thermocline), 15-30 m (layer of seasonal ther-

mocline), and 30-60 m (lower part of seasonal thermocline, lower part of isohaline layer). The mean observed values in these layers are shown in Fig. 5. The highest mean concentrations occurred last winter (March) and equalled over 7.6 mmol m⁻³ at station A and 5.9 mmol m⁻³ at station B. The lowest concentrations in the upper layer occurred at the beginning of May at A and in middle May at B and equalled 0.57 mmol m⁻³ at A and 0.74 mmol m⁻³ at B. At station A inorganic nitrogen depletion, with concentrations < 1 mmol m⁻³, occurs in the upper 30 m at the beginning of May, but at B it is encountered about one month later (ca. 20 days).

However, samples of phosphate taken from water also were collected in determined layers: 0-15, 15-30, and 30-60 m. The mean observed values in these layers are shown in Fig. 6. The highest mean concentrations of phosphate occurred last winter (March) as in the case of inorganic nitrogen, which equalled over 0.68 mmol m⁻³ at station A and 0.52 mmol m⁻³ at B. The lowest concentrations in the upper layer occurred late April at A and in May at B and equalled 0.007 mmol m⁻³ and 0.009 mmol m⁻³, respectively, at stations A and B. At station A phosphate depletion, with concentrations < 0.01 mmol m⁻³, occurs in the upper 15 m in late April, but at B it is encountered about one month later (ca. 25 days). The conversions, g , from N and P to carbon which are applied in equations (see Appendix for nutrients) are given in Table 2 as g_N and g_P .

The differences between the simulated and mean observed values of nutrients in the upper layer (0-15 m) are about 0.5-1 mmol m⁻³ for total inorganic nitrogen and ca. 0.1 mmol m⁻³ for phosphate (Fig. 7). The total inorganic nitrogen is the major factor controlling the biomass of phytoplankton in the Baltic Sea after [27], although cyanobacteria overcome N shortage by N-fixation and primary production in the end is limited

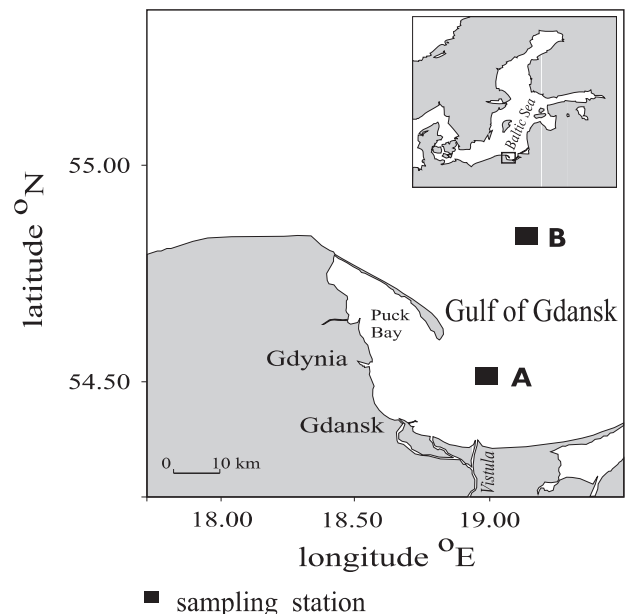


Fig. 2. Map of Gdańsk Gulf showing sampling stations.

by available phosphorus. Shaffer [27] determined the phosphate-to-nitrogen ratio for Baltic Sea water as $P/N=1:14.4$. However, [28] obtained the relationship of phosphate concentrations and the total concentration of inorganic nitrogen in the euphotic layer in the southern Baltic Sea as $P=0.072N+0.115$. This equation suggests

that in the vegetation season, the P/N ratio is equal to 1:14.1. In the Gdańsk Gulf in this period, the N/P ratio is equal to 10.8; but in the Gdańsk Deep, it is 6.5 after [28]. In my opinion, P/N ratio during vegetation period tends to zero or infinity because either N or P is close to zero.

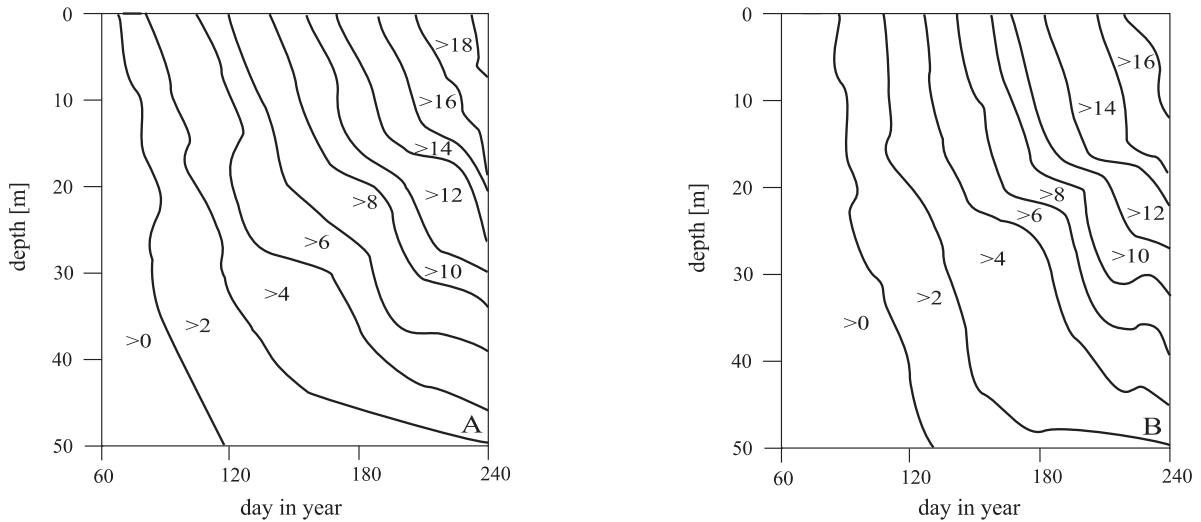


Fig. 3. Simulated temperature profiles at stations A and B.

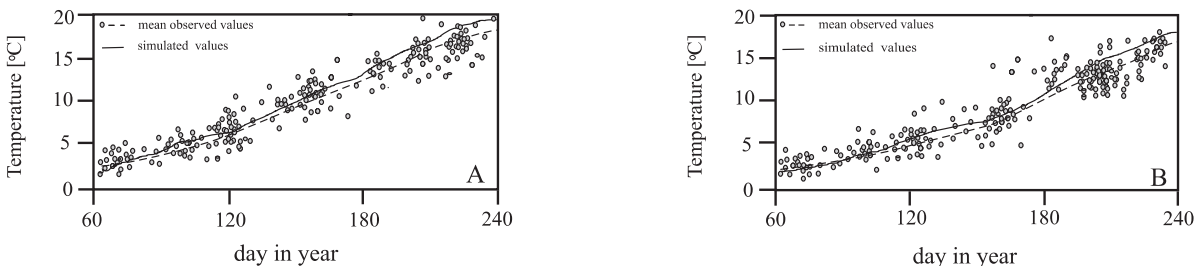


Fig. 4. Simulated and mean observed values of surface temperature at stations A and B.

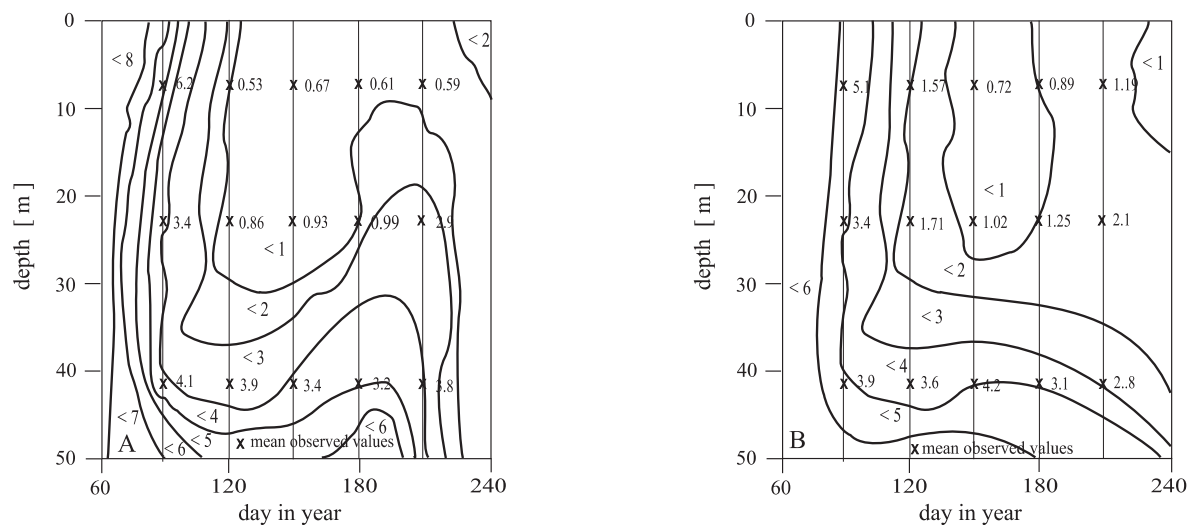


Fig. 5. Simulated profiles and observed values of total inorganic nitrogen at A and B.

The phytoplankton biomass reflects nutrient availability, showing a strong nutrient-depleting spring bloom (Fig. 8). At station A, the phytoplankton biomass reached maximum values from 350 mgC m⁻³ on the surface to 50 mgC m⁻³ at depth; contrasting the range from 200 to 50 mgC m⁻³ at station B. Hence, {Phyt} was about two times higher in the surface layer at station A than at B. The differences in {Phyt} between the two stations decreased with depth.

This situation is caused by high nutrient concentration near the river mouth (where its influence on the values of the biological characteristics investigated is visible) as well as by the water temperature which was higher at station A than at B. Temperature data was used for the primary production calculation, which is the dominant process determining the pattern of phytoplankton biomass.

Phytoplankton biomass is more often measured as chlorophyll-*a* than as carbon. From April to May, in the spring bloom time, chlorophyll ranges from nearly 7 to about 20 mgChl m⁻³ at the surface sea in the Gdańsk Gulf. Mean high concentrations are found at station A ca. 360 mgC m⁻³ and at B ca. 250 mgC m⁻³ (Fig. 9). To compare the simulated results for phytoplankton carbon to available chlorophyll-*a* data, a C/Chl-*a* ratio has to be assumed for converting the simulated carbon contents to chlorophyll-*a*. Here, the calculations were made assuming the C/Chl-*a* ratio is equal to ≈34 mgC (mgChl)⁻¹ as mean value for the southern Baltic Sea in the upper layer [28]. Then, the differences in the *Phyt* between the modelled and mean observed values are ca. 3-15% of the maximum value.

Fig. 10 demonstrates the simulated profiles of zooplankton biomass {Zoop} at stations A and B. Tempo-

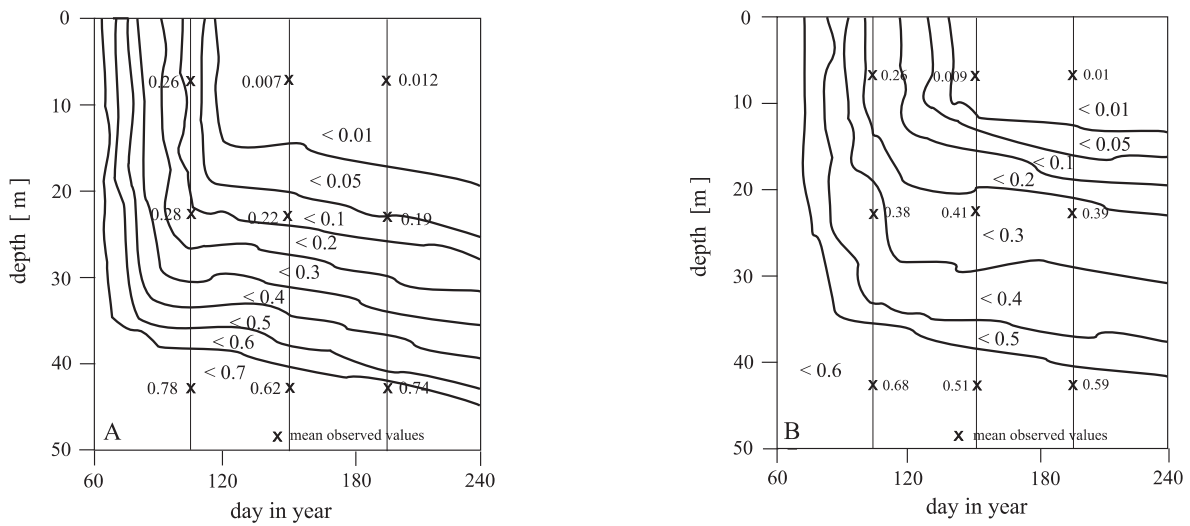


Fig. 6. Simulated profiles and observed values of phosphate at stations A and B.

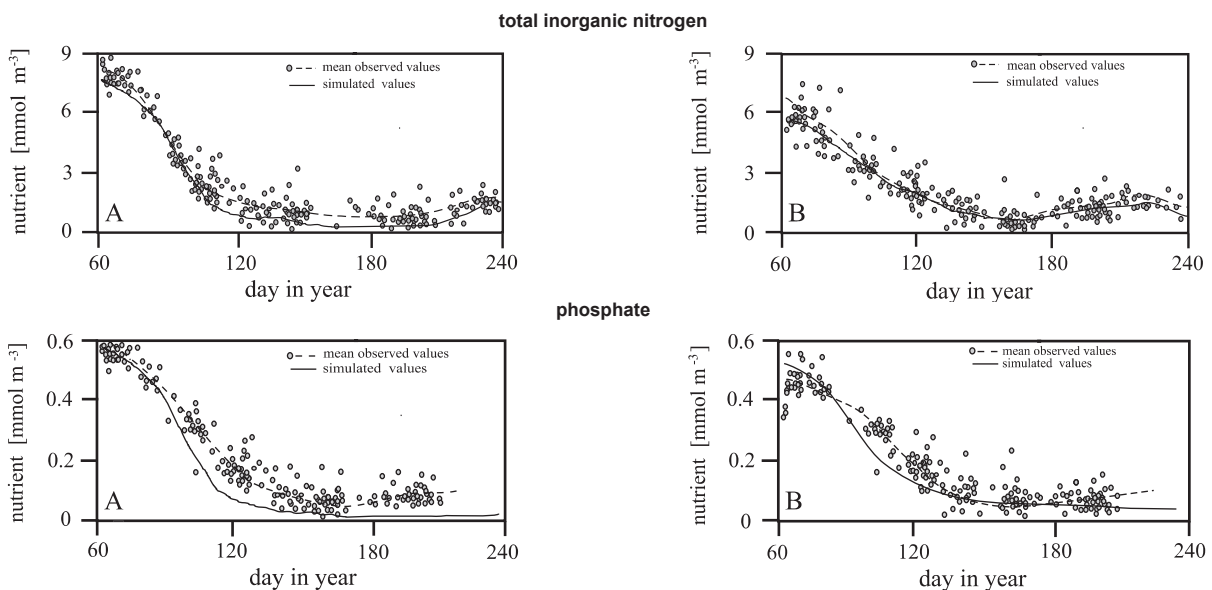


Fig. 7. Simulated and mean observed values of total inorganic nitrogen and phosphorus in the upper layer at stations A and B.

ral variability of {Zoop} are different at both stations. The zooplankton reached maximum values from about 75 mgC m⁻³ on the surface to 5 mgC m⁻³ at depth in May at A and from 50 to 2 mgC m⁻³ in June at B. However, in

March {Zoop} reached about 2 mgC m⁻³ at A and 1 mgC m⁻³ at B in the whole water column.

The results of the numerical simulations for depth integrated zooplankton biomass described here are compared

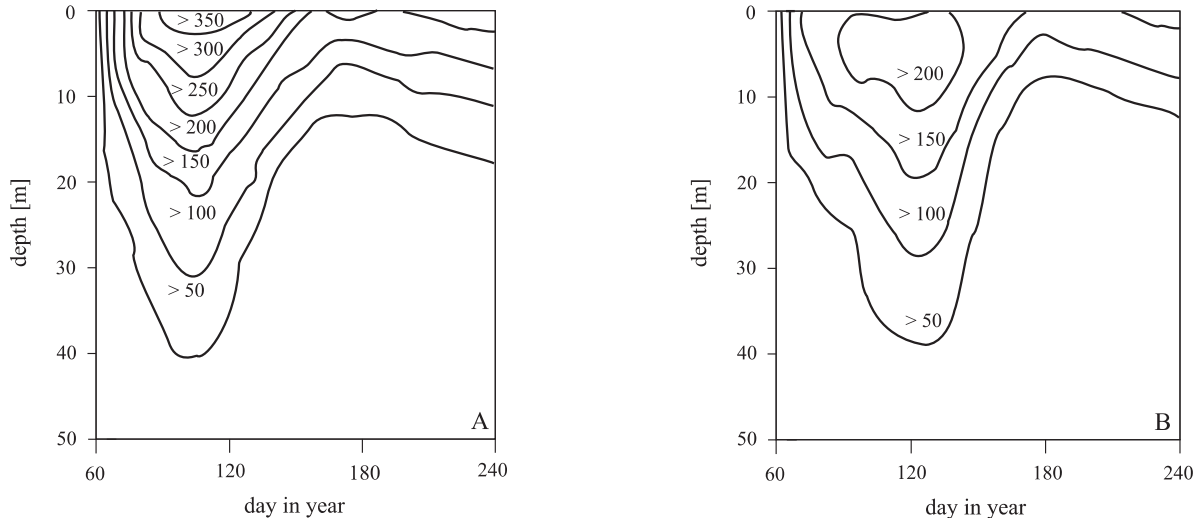


Fig. 8. Simulated profiles of phytoplankton biomass at stations A and B.

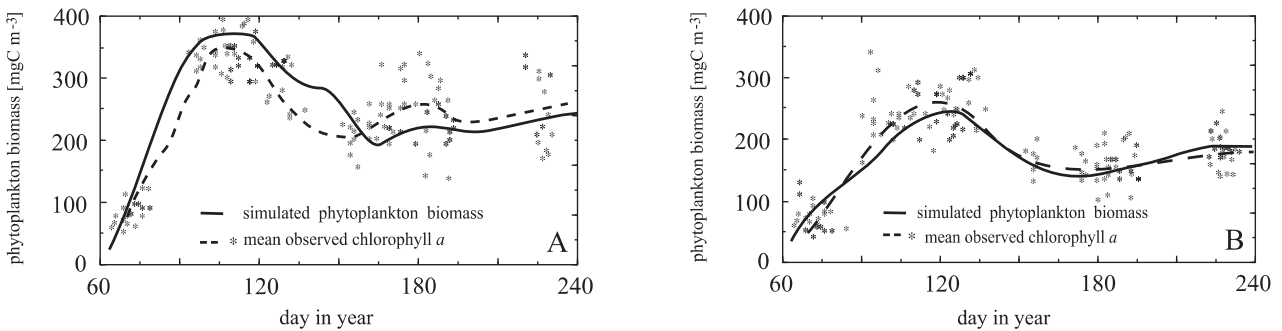


Fig. 9. Simulated and observed values of phytoplankton at the surface sea at A and B.

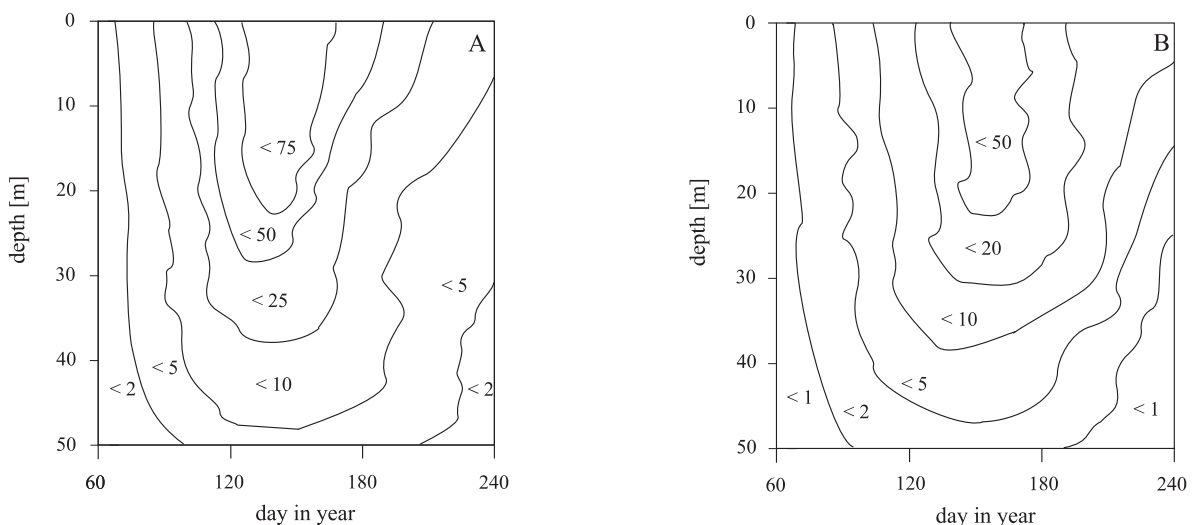


Fig. 10. Simulated profiles of zooplankton biomass at stations A and B.

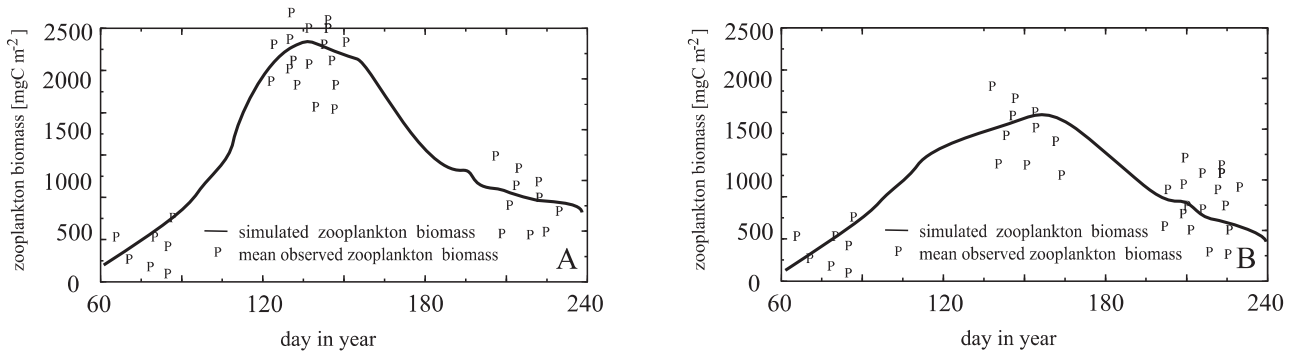


Fig. 11. Simulated and observed values of depth integration of zooplankton at A and B.

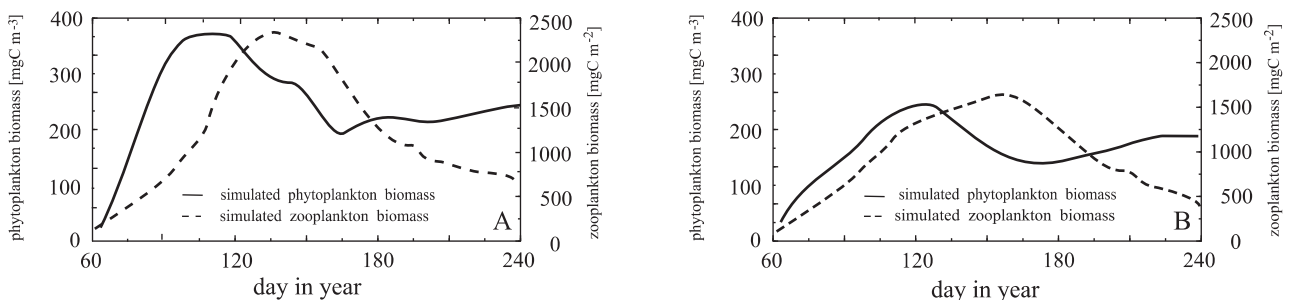


Fig. 12. Phytoplankton biomass in the surface layer and depth-integrated zooplankton biomass at stations A and B.

with the mean observed values assuming organic carbon content of $\text{gC/g}_{\text{w.w.}} = 0.11$ [29] (Fig. 11). The mean high value of zooplankton biomass during the period of simulation was observed in the end of May (ca. $18 \text{ g}_{\text{w.w.}} \text{ m}^{-2}$) in Gdańsk Gulf and it corresponds to ca. 2 gC m^{-2} . It is similar to the value calculated here, i.e. $\{Zoop\} \approx 2.3 \text{ gC m}^{-2}$ at A and $\{Zoop\} \approx 1.7 \text{ gC m}^{-2}$ at B. Comparing depth, integrated zooplankton biomass from the calculated and mean experimental data, the present results indicate that the difference in the $\{Zoop\}$ is ca. 5-20% of the maximum value.

Fig. 12 presents the changes in phytoplankton biomass in the surface layer and depth integrated zooplankton biomass. The simulations show the general variations in populations with time. The results are significant changes in distributions of phytoplankton and zooplankton biomass which have taken place in an area of considerable increase of primary production and grazing. In the initial stage of the numerical experiment, a substantial growth of phytoplankton biomass is observed, which slightly falls at the next stage as a result of an increase of zooplankton biomass. This growth is caused by an increase of grazing of phytoplankton by zooplankton.

Conclusion

This work presents the one-dimensional model to simulate the temporal changes in distributions of a nutrient, phytoplankton and zooplankton and study the role of these biological characteristics in the dynamics of the Gdańsk Gulf ecosystem. Models are suitable as tools be-

cause hypothesis can be tested, and our understanding of processes and dynamics can be evaluated.

The simulated biological characteristics (i.e. the inorganic nitrogen and phosphate, the surface phytoplankton biomass and depth integrated zooplankton biomass) in the model were compared to the observations from the investigated water regions. Taking into consideration the fact that outputs of the meteorological submodel were obtained using meteorological data for 1998 and climatological data, the comparison of numerical results will be made to the mean values of empirical data for a period of 10 years (1990-2000). Most data exist for 1998 from Gdańsk Deep.

The numerical simulations shown that the differences between the simulated and mean observed values of nutrient in the upper layer are ca. 1 mmol m^{-3} for total inorganic nitrogen and ca. 0.1 mmol m^{-3} for phosphate. At station A inorganic nitrogen depletion with concentrations $< 1 \text{ mmol m}^{-3}$ occurs in the upper 30 m layer; however, phosphate depletion with concentrations $< 0.01 \text{ mmol m}^{-3}$ occurs in the upper 15 m layer in late April. At station B, it is encountered on month later. Phytoplankton biomass reflects nutrient availability, showing a strong nutrient-depleting spring bloom at station A. $\{Phyt\}$ was about 2 times higher in the surface layer at station A than at B. This situation is caused by the high nutrient concentration near the river mouth (where its influence on the values of biological characteristics is visible).

Fig. 9 presents the observed mean values of surface chlorophyll-*a* for stations A and B (Regional Oceano-

graphic Database of IOPAS). The chlorophyll-*a* values shown for these areas were obtained from water samples. At open sea station chlorophyll-*a* concentration was lower than in the gulf. A considerable proportion of chlorophyll-*a* variability at the investigated points results solely from variations in weather conditions and nutrient distributions. To compare the simulated results for phytoplankton carbon to available chlorophyll-*a* data, a C/Chl-*a* ratio has to be assumed for converting the simulated carbon contents to chlorophyll-*a*. Literature mean value for the C/Chl-*a* ratio lie between 31.06 for open water of the southern Baltic Sea and 42.85 for coast water in the upper layer (see Table 1 in paper [28]). However, in this paper the calculations were made assuming the C/Chl-*a* ratio $g_{Chl} = 34.31 \text{ mgC}(\text{mgChl})^{-1}$ as mean value for the southern Baltic Sea [28]. Thus, in the surface layer, the mean observed value of the maximum chlorophyll-*a* content ca. $10.3 \text{ mgChl m}^{-3}$ at A and ca. 8.2 mgChl m^{-3} at B corresponds to 353 mgC m^{-3} and 251 mgC m^{-3} , respectively. These chlorophyll data and the simulated phytoplankton biomass are well correlated during the period of simulation and attain their maximum concentrations in April, which are of similar magnitude, depending on the conversion factor C/Chl-*a*. However, the maximum of the simulated blooms occurs a few days earlier at A and later at B than in the measurements. The difference in the $\{Phyt\}$ between the modelled and mean observed values is equal to 0.5-1.3 mgChl m^{-3} and depends on the month for which the calculations were made.

The results of the numerical simulations for depth integrated zooplankton biomass described here were compared with the mean observed values assuming organic carbon content of microzooplankton $gC/g_{w.w.} = 0.11$. The biomass peak of microzooplankton in Gdańsk Deep appears in late spring (about $11 \text{ g}_{w.w.} \text{ m}^{-2}$); however, the mean annual biomass of is about $15 \text{ g}_{w.w.} \text{ m}^{-2}$. The highest value of microzooplankton biomass during the period of simulation was observed in the end of May (about $17 \text{ g}_{w.w.} \text{ m}^{-2}$) and it corresponds to 1900 mgC m^{-2} . It is higher value than here calculated. Comparing the depth integrated microzooplankton biomass from the calculated and mean experimental data, the present results indicate that the difference in the $\{Zoop\}$ is equal to 0.2-0.5 gC m^{-2} at these stations.

The simulations given here show that in the Gulf of Gdansk, in the final stage of spring bloom (May) nutrient limitation in the surface layer and zooplankton growth tends to a decrease of phytoplankton concentration in the open area. In the coastal area concentration is still high.

The high variability of phytoplankton concentration in the longitudinal direction is well known from observations.

The results of the numerical simulations described here are in good agreement with the mean observed values. The 1D-ecosystem model can be utilized for numerical investigations of phytoplankton, microzooplankton biomass and nutrients distributions.

Acknowledgements

This research was carried out as part of statutory programme of the Institute of Oceanology in Sopot, Poland (No. II.1.) and was supported by the Polish State Committee of Scientific Research (grant No 2PO4F 075 27, 2004-2006).

Appendix

Parameters of the Biological Submodel

NUTRIENTS

$$\begin{aligned} \text{REL} &= g\text{RES}, \quad \text{UPT} = g(\text{PRE} - \text{RES}) \\ \text{EXC} &= g\text{MET} = g(M_s + n_e A) \\ \text{FEC}_z &= n_f \text{GRA}, \quad \text{MOR}_z = n_z \text{GRA} \\ \text{REMP} &= p_p \text{MOR}_p, \quad \text{REMZ} = p_z \text{MOR}_z, \quad \text{REMF} = p_f \text{FEC}_z \\ \text{REMI} &= g(\text{REMP} + \text{REMZ} + \text{REMF}) \\ &= g \left\{ p_p \text{MOR}_p + (p_f n_f + p_z n_z) \text{GRA} \right\} \\ F_{\text{inf}} &= F_{\text{inf},0} \exp(-0.1z) \end{aligned}$$

PHYTOPLANKTON

$$\begin{aligned} \text{PRE} &= \sin \gamma d_i d_j \min\{d_p, d_N\} \{Phyt\} \\ d_i &= \frac{E}{E_o} \exp\left(1 - \frac{E}{E_o}\right), \quad d_p = \frac{\{Nutr_P\}}{\{Nutr_P\} + k_{Nutr_P}}, \quad d_N = \frac{\{Nutr_N\}}{\{Nutr_N\} + k_{Nutr_N}} \\ E_o &= 313.64 + 19.56 T; \quad d_A = 1.385 + 0.238 T \end{aligned}$$

$$\begin{aligned} E &= \frac{\eta_d}{d} \exp(-K_d z) \left(1 + \cos \frac{2\pi z}{d}\right) \\ \eta_d &= 8.67 + 8.29 \cos(\omega x - 3.03) + 0.69 \cos(\omega x - 5.80) \\ \text{RES} &= \text{RES}_s + \text{RES}_d = d_A (m_p^s + m_p^d \min\{d_i, d_N\}) \{Phyt\} \end{aligned}$$

$$\begin{aligned} \text{MOR}_p &= m_p \{Phyt\} \\ \text{GRA} &= g_{\text{max}} \frac{\{Phyt\} - \{Phyt\}_0}{\{Phyt\} - \{Phyt\}_0 + k_{Phyt}} \{Zoop\} \text{ for } \{Phyt\} > \{Phyt\}_0 \end{aligned}$$

ZOOPLANKTON

$$\begin{aligned} \text{ING} &= \tau \text{fil}(\{Phyt\}) \{Zoop\} \\ \text{fil}(\{Phyt\}) &= \text{fil} \frac{\{Phyt\} - \{Phyt\}_0}{\{Phyt\} - \{Phyt\}_0 + k_{Phyt}} \end{aligned}$$

$$\begin{aligned} \text{MET} &= M_s + M_r + M_d = M_s + n_e A, \quad A = n_a \text{ING} \\ \text{PRED} &= \{Zoop\} \exp(-m_z t) \end{aligned}$$

BENTHIC DETRITUS

$$\begin{aligned} \text{SEDI} &= (1 - p_p) \text{MOR}_p + (1 - p_f) \text{FEC}_z + (1 - p_z) \text{MOR}_z \\ &= (1 - p_p) \text{MOR}_p + \left\{ (1 - p_f) n_f + (1 - p_z) n_z \right\} \text{GRA} \\ D &= \int_0^H \text{SEDI} dz \\ \text{REMD} &= r_d \{Detr\} \end{aligned}$$

References

1. SVANSSON A. The Baltic circulation. A review in relation to ICES/SCOR Task 3. In: Proceedings of the 10th Conference of the Baltic Oceanography. Göteborg, Sweden, **1976**.
2. SVANSSON A. Long-term variations in the Kattegat hydrography. ICES COUNCIL MEETING 1984 (Collected papers), Copenhagen, 13, **1984**.
3. SVANSSON A. Review of the hydrographical Joint Skagerrak Expedition in 1966. ICES COUNCIL MEETING 1989 (Collected papers), Copenhagen, 14, **1989**.
4. SVANSSON A. A diffusion model for the primary production of phytoplankton. Deep-Sea Res. II **43** (1), 37, **1996**.
5. FRANZ H., MOAMMERTS J., RADACH G. Ecological modelling of the North Sea. Neth. J. Sea Res. **28** (172), 67, **1991**.
6. FRANZ H.G., GONZALEZ S.R., STEENEKEN S.F. Metazoan plankton and the structure of the plankton community in the stratified North Sea. Mar. Ecol. Prog. Ser. **175**, 191, **1998**.
7. RADACH G. Simulations of phytoplankton dynamics and their interaction with other system components during FLEX'76. In: J. Sundermann, W. Lenz (Editors), North Sea Dynamics. Springer-Verlag, Berlin, Heidelberg, New York, pp. 584-632, **1983**.
8. RADACH G., MOLL A. Estimation of the variability of production by simulating annual cycles of phytoplankton in the central North Sea. Prog. Oceanogr. **31**, 339, **1993**.
9. MOLL A., RADACH G. Review of three-dimensional ecological modelling related to the North Sea shelf system: Part I. Models and their results. Prog. Oceanogr. **57** (2), 175, **2003**.
10. FONSELIUS S.H. Hydrography of the Baltic deep basins III-Fishery Board of Sweden. Ser. Hydrogr. **29**, 1, **1969**.
11. JANSSON B. Ecosystem approach to the Baltic problem. Bull. Res. Committee NFR **16**, 1, **1972**.
12. STIGEBRANDT A., WULFF F. A model for the dynamics of nutrients and oxygen in the Baltic Proper. J. Mar. Res. **45**, 729, **1987**.
13. SAVCHUK O., KOLODOCHKA A., GUTSABBATH E. Simulation of the matter cycle in the Baltic Sea ecosystem. Proceedings of the 16th Conference on Baltic Oceanography. Kiel, pp. 921-931, **1988**.
14. ENNET P., KINNUNEN K., TAMSALU R. Ecosystem model FINEST. Valgus Tallinn, **1989**.
15. TAMSALU R., ENNET P. Ecosystem modelling in the Gulf of Finland. II. The aquatic ecosystem Model FINEST. Estuar. Coast. Shelf Sci. **41**, 429, **1995**.
16. DZIERZBICKA-GŁOWACKA L. Mathematical modelling of the biological processes in the upper layer of the sea. Diss. and monogr. 13, Institute of Oceanology PAS, Sopot, 124, **2000** (in Polish).
17. CARLOTTI F., RADACH G. Seasonal dynamics of phytoplankton and *Calanus finmarchicus* in the North Sea as revealed by a coupled one-dimensional model. Limnol. Oceanogr., **41** (3), 522, **1996**.
18. CARLOTTI F., WOLF K.U. A Lagrangian ensemble model of *Calanus finmarchicus* coupled with a 1D ecosystem model. Fish. Oceanogr. **7** (3/4), 191, **1998**.
19. DZIERZBICKA-GŁOWACKA L. A numerical investigation of phytoplankton and *Pseudocalanus elongatus* dynamics in the spring bloom time in the Gdańsk Gulf. J. Mar. Sys. **53**, 19, **2005**.
20. CARLOTTI F., NIVAL P. Model of copepod growth and development: moulting and mortality in relation to physiological processes during an individual moult cycle. Mar. Ecol. Prog. Ser. **84**, 219, **1992**.
21. DZIERZBICKA-GŁOWACKA L. Growth and development of copepodite stages of *Pseudocalanus* spp. J. Plankton Res. **26** (1), 49, **2004**.
22. PETERS H., GREGG M.C., TOOLE M.I. On the parametrization of equatorial turbulence. J. Geophys. Res. **93**, 216, **1988**.
23. FRIEDRICH H.J., KOCHERGIN V.P., KLIMOK V.I., PROTASOV A.V., SUKHORUKOV V.A. Numerical experiments for the model of the upper oceanic layer. Meteorologija Hidrologija **7**, 77, **1981**.
24. KOCHERGIN V.P., KLIMOK V.I., SUKHORUKOV V.A. A turbulent model of the ocean Ekman layer. Sbornik Chislennich Metody Mekhaniki Sploshnoi Sredy **7**, 72, **1976**.
25. POTTER D. Computation Physics. Wiley, London, New York, Sydney, Toronto, **1982**.
26. CYBERSKA B., LAUER Z., TRZOSIŃSKA A. Environmental conditions in the Polish zone of the southern Baltic Sea during 1998. Institute of Meteorology and Water Management. 288, **1999** (in Polish).
27. SHAFFER G. Redfield rations, primary production and organic carbon burial in the Baltic Sea. Deep Sea Res. **34**, pp 769-784, **1987**.
28. RENK H. Primary production in the southern Baltic. Stud. Mat. A **35**, Sea Fisheries Institute, Gdynia, 78, **2000** (in Polish).
29. EDLER L. Recommendation on methods of marine biological studies in the Baltic Sea. Phytoplankton and chlorophyll. BMB publ. 5, Univ. Lund. **1979**.